Provided for non-commercial research and education use.
Not for reproduction, distribution or commercial use.

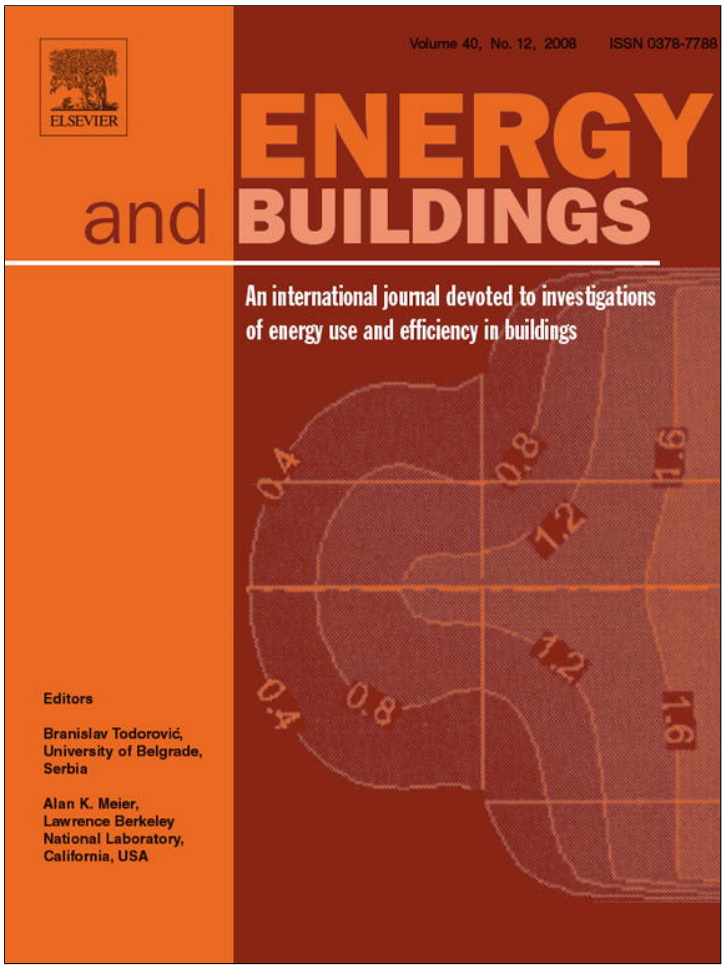

This article appeared in a journal published by Elsevier. The attached copy is furnished to the author for internal non-commercial research and education use, including for instruction at the authors institution and sharing with colleagues.

Other uses, including reproduction and distribution, or selling or licensing copies, or posting to personal, institutional or third party websites are prohibited.

In most cases authors are permitted to post their version of the article (e.g. in Word or Tex form) to their personal website or institutional repository. Authors requiring further information regarding Elsevier's archiving and manuscript policies are encouraged to visit:

http://www.elsevier.com/copyright

Author's personal copy

Energy and Buildings 40 (2008) 2099–2110

Contents lists available at ScienceDirect

Energy and Buildings

journal homepage: www.elsevier.com/locate/enbuild

The response of natural displacement ventilation to time-varying heat sources

Diogo Bolster *, Alex Maillard, Paul Linden

Department of Mechanical and Aerospace Engineering, University of California, San Diego, USA

ARTICLE INFO

Article history:
Received 1 June 2007
Received in revised form 18 April 2008
Accepted 2 June 2008

Keywords:
Natural ventilation
Transient

ABSTRACT

We examine transients caused by sudden changes in heat load in a naturally ventilated chamber. The space we consider has an isolated heat source, modeled as an ideal plume, and is connected to the exterior via openings at the top and bottom. Pressure differences between the exterior and interior that arise due to the buoyancy in the space drive a natural ventilation flow through the space that generates a two-layer system with buoyant (warm) fluid in the upper layer and ambient fluid in the lower layer. We develop two mathematical models, one assuming perfect mixing of each layer, the other accounting for stratification. We compare both models to small scale laboratory experiments. Neither model is significantly better than the other, and both give good agreement with the experiments.

Using these models we identify many appealing features of the type of natural ventilation studied here. These include the fact that a well designed system is self-controlling. The manner in which it controls itself is very robust, because the larger the change in heat load the faster the system will readjust. Also there is a resistance against the interface penetrating deeply into the occupied zone, even for very large changes in heat load.

© 2008 Elsevier B.V. All rights reserved.

1. Introduction

With the ever growing awareness for a need to protect the environment it has become increasingly important to find ways to reduce the rapidly growing global energy consumption. About one-third of the world's energy is used by building services, of which a significant portion is expended on ventilation. A better understanding of ventilation is necessary in order to design and operate more efficient ventilation systems. Knowledge of the manner in which air mixes within buildings is key to the design of better control systems and ventilation schemes can be designed.

Many heat sources can be regarded as localised and understanding the manner in which they stratify a space is critical to the design of energy efficient ventilation schemes. Localised heat sources may often be modeled as an ideal plume (i.e. a pure source of buoyancy, e.g. a radiator, computer, person). Several ventilation processes can be modeled and better understood by looking at the flow produced by such a localised source of buoyancy in a confined space. The problem is critical for natural ventilation in buildings, where convective flows dominate [15].

Motivated by this and similar problems, much work has been done looking at the flow generated by a buoyant plume within a confined space. The plume is modeled using the classical plume theory developed by Morton et al. [19]. They model the plume with three conservation equations for volume flux, momentum flux and buoyancy flux. The system of equations is closed with the powerful entrainment assumption, which assumes that the velocity of fluid being entrained into the plume is proportional to a characteristic vertical velocity in the plume. Baines and Turner [1] studied the interaction of a buoyant plume and the background environment in a closed space. They considered the flow that develops when an isolated source of buoyancy alone issues into the closed space. This model has come to be known as the 'filling box' model.

Germeles [10] developed a sophisticated, yet simple, numerical algorithm to study the 'filling box' model. With this algorithm it is possible to resolve the transient evolution of the stratification in a space quickly and accurately with little computational expense. In this scheme the background ambient fluid is discretized into a finite number of layers, n, and it is assumed that the plume evolves on a faster time-scale than the ambient. Therefore, for any given time step, the equations associated with the plume are solved in a quasi steady fashion assuming that the background does not vary. Once the plume equations have been solved the background layers, whose concentration and density remain unchanged during a particular time-step, are advected with a velocity that can be calculated from volume conservation. This process captures the entrainment of fluid from each layer by the rising plume since the advected layers reduce in thickness at each time step. At each

* Corresponding author. Tel.: +1 858 405 1014.
E-mail address: diogobolster@gmail.com (D. Bolster).

0378-7788/$ – see front matter © 2008 Elsevier B.V. All rights reserved.
doi:10.1016/j.enbuild.2008.06.001

Author's personal copy

timestep a new layer is added, the thickness of which is determined by the flow rate of the plume at the top of the room and size of the chosen time step. The density assigned to this new layer is the same as the density of fluid in the plume at the top of the room.

Killworth and Turner [13] studied the filling box model in an enclosed space for a pure plume with a time varying buoyancy flux. They noted that as long as the plume buoyancy flux at every height is larger than the buoyancy in the background of the room the plume can penetrate the whole way through the space and spread at the top. However, if the source buoyancy flux is not sufficiently large, the plume becomes a fountain above the level of zero relative buoyancy, which stops rising at the level of zero momentum. It will then fall back and spread horizontally at some height between these two levels. Killworth and Turner found that modeling the spread of the plume at the level of zero buoyancy better matched their experimental data than at the level of zero momentum. Similar observations were made by Kumagai [14] and Cardoso and Woods [4], who studied the 'filling box' model for a room which has some ititial background stratification.

Linden et al. [16] opened Baines and Turner's filling box to the ambient by placing vents in the box that allowed a flow driven by buoyancy differences between the interior and exterior to develop through the space. They primarily studied the steady states that developed for constant strength point, line and vertically distributed sources. These are extensions of the filling box model, with the addition of a continuous exchange between the internal and external environments. This 'emptying filling box' model is often used to model natural ventilation. Their results show that a two layer system develops in the room with ambient fluid beneath the interface and buoyant fluid above it. For an ideal plume source, the height of the dividing interface depends only on the area of the vents and not the source buoyancy flux.

Kaye and Hunt [12] studied the initial transient that evolves in the 'emptying filling box' when the heat source is initially turned on. As in Linden et al. [16], they showed that the steady state flow is characterized entirely by a dimensionless vent area. They identified that for certain values of this vent area the depth of the buoyant upper layer may overshoot the steady layer depth during the initial transient. They also determined the critical value of the dimensionless area for this overshoot to occur.

Other than Kaye and Hunt [12] most natural ventilation models ('emptying filling boxes') only consider the steady states associated with the flow. The work presented here extends these models by considering a heat source whose buoyancy flux changes at some time. Specifically, we consider the situation where there is a sudden change in source buoyancy flux, which could correspond a piece of equipment being turned on/off or people entering/exiting a room.

Assessing the viability of natural ventilation, due to many competing criteria such as noise, air quality and energy savings, is a complicated task, which must consider climate, specific location and purpose of the space in question (e.g. [9]). Potential energy savings are often cited as being one of the main benefits of natural ventilation, but again it is difficult to quantify without detailed information of the space being ventilated. Many useful simulation tools such as the US Department of Energy code EnergyPlus [7] and [8] exist that can provide useful quantitative data. Successful use of such codes requires the integration of accurate ventilation models. The integration of models based on similar principles to the one presented herein (e.g. [17,18]) has proven useful in providing more accurate results than the use of traditional models [2]. The work presented herein aims to provide further useful information that could, if deemed necessary, be used as input into such ventilation modeling programs.

In Section 2 of this paper we describe the mathematical model applicable to the above case. We consider a case starting from some initial steady state, then change the source buoyancy flux and observe the transition to the next steady state. In Section 3 we present and discuss the results from the model described in Section 2. Section 4 considers the limitations of the well-mixed assumption in our model, by considering a model that does account for stratification and comparing the results of these two models and in Section 5 we present the results of laboratory experiments.

2. Well-mixed model

Fig. 1 is a schematic depicting a two-layer well-mixed model for natural ventilation. A heat source is represented by a single ideal plume (i.e. no source volume and momentum flux) located on the floor. Linden et al. [16] showed that at steady state the stratification has two uniform layers separated by an interface. The height h of this interface depends only on the area of the inlet and outlet vents and not on the source buoyancy flux of the plume. This is one of the features of natural ventilation that is so appealing. It is a self-controlling system that will provide the same temperature in the lower layer regardless of the strength of the heat source. Since typically, the lower layer is the only one that is occupied and the temperature of the upper layer is relatively unimportant from a comfort perspective, this property makes natural displacement ventilation very robust.

As mentioned, all of the above assumes steady state. However, most realistic sources are not steady. If the buoyancy flux of the source is varying over time this will in turn cause the interface height h to change. As the new steady state is attained the interface will settle back to its original height. We are interested in determining the temporal variation of this interface between these two steady states where the initial and final interface heights are the same.

A key assumption of the model depicted in Fig. 1 is that the buoyant upper layer is well mixed at all times. While the layers are uniform at steady state, a change in buoyancy flux is expected to produce a temporary stratification in the upper layer. For the moment we will ignore this stratification and assume that both layers remain uniform in temperature as they evolve. From our experimental observations it is evident that this assumption is not strictly valid and that during the transitions from one steady state to the next some stratification will evolve in the upper layer. Kaye

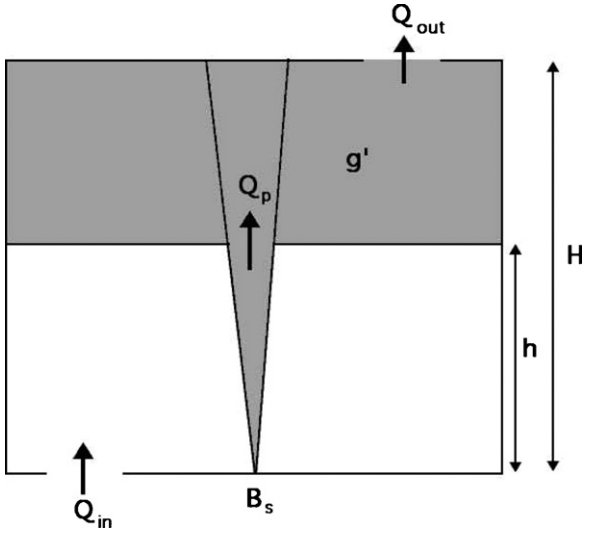

Fig. 1. Natural ventilation with a single ideal plume heat source.

Author's personal copy

and Hunt [12] suggest that the only source of error of this assumption should be to underpredict the buoyancy of the fluid leaving the box, which in turn will lead to an underprediction for the time taken for the buoyancy of the layer to reach a steady state. They also argue that there will be some level of mixing in the upper layer due to the finite thickness outflow from the top of the plume.

By assuming that the upper and lower layer are well mixed at all times the system can be fully described by two conservation equations that are coupled, nonlinear ODEs. The conserved quantities we consider are the volume and buoyancy of the upper layer.

2.1. Conservation of volume

The volume flow rates in and out of the room (Fig. 1) are always equal

$$Q_{\text{in}} = Q_{\text{out}}, \tag{1}$$

Therefore, applying conservation of volume to the upper layer ($y > h$) in the chamber leads to

$$\frac{\mathrm{d}V}{\mathrm{d}t} = Q_{\text{p}} - Q_{\text{out}}, \tag{2}$$

where V is the volume of the upper layer and Q_{p} is the volume flux of the plume at the interface height.

Using Bernoulli's equation it can be shown that the flow rate in and out of the room is

$$Q_{\text{out}} = A^* \sqrt{g'(H-h)}. \tag{3}$$

where A^* is the weighted area of the upper and lower openings as in [16]. A^* includes the loss coefficient for both the upper and lower openings, which links the physical size and geometry of these ventilation openings. The reduced gravity of the upper layer is defined as

$$g' = g\frac{\rho - \rho_a}{\rho_a}. \tag{4}$$

Since the lower layer is uniform, Q_{p} can be calculated using the solution for an ideal plume in an unstratified environment developed by Morton et al. [19]

$$Q_{\text{p}} = cB^{1/3}z^{5/3}, \tag{5}$$

where B is the source buoyancy flux and c is a constant based on the plume entrainment constant. Substituting Eqs. (5) and (3) into Eq. (2) results in an equation for the evolution of the interface height

$$\frac{\mathrm{d}h}{\mathrm{d}t} = \frac{A^*\sqrt{g'(H-h)}}{S} - \frac{cB^{1/3}z^{5/3}}{S}, \tag{6}$$

where S is the cross-sectional area of the room.

2.2. Conservation of buoyancy

The conservation of buoyancy of the upper layer can be written as

$$\frac{\mathrm{d}g'V}{\mathrm{d}t} = B_{\text{p}} - Q_{\text{out}}g', \tag{7}$$

where B_{p} is the buoyancy flux of the plume at the interface. Because the lower layer is unstratified B_{p} and B, the source buoyancy flux, are equal. Using this fact and substituting Eq. (3) into Eq. (7), conservation of buoyancy can be reduced to

$$\frac{\mathrm{d}g'}{\mathrm{d}t} = \frac{1}{S(H-h)}[B - cg'B^{1/3}h^{5/3}]. \tag{8}$$

2.3. Sudden change in buoyancy

We consider a sudden discontinuous change in the source buoyancy flux from some initial steady value B_0 to a different value $B_0 + \Delta B$, where ΔB can be positive or negative, corresponding to an increase or a decrease in buoyancy from the heat source.

Let us introduce two dimensionless parameters

$$\zeta = \frac{z}{H}, \quad \delta = g'\frac{cH^{5/3}}{B_u^{2/3}}. \tag{9}$$

where ζ represents a dimensionless interface height and δ a dimensionless reduced gravity. For natural ventilation, two important time scales are typically considered. These are the draining, T_{d}, and filling, T_{f}, time scales, defined in Eq. (10) below and are the same as the timescales defined in [12]. In this present situation there are four time scales since there will be two draining and two filling times, corresponding to the initial and final source buoyancy fluxes.

For the initial buoyancy flux B_0

$$T_{\text{d1}} = \frac{c^{1/2}SH^{4/3}}{A^*B_0^{1/3}}, \quad T_{\text{f1}} = \frac{S}{cB_0^{1/3}H^{2/3}}. \tag{10}$$

Similarly, for the final buoyancy flux $B_0 + \Delta B$

$$T_{\text{d2}} = \frac{c^{1/2}SH^{4/3}}{A^*(B_0+\Delta B)^{1/3}}, \quad T_{\text{f2}} = \frac{S}{c(B_0+\Delta B)^{1/3}H^{2/3}}. \tag{11}$$

When $B = B_0$, and using the dimensionless parameters introduced in Eqs. (9), (6) and (8) reduce to the relations presented by Kaye and Hunt [12], namely

$$\frac{\mathrm{d}\zeta}{\mathrm{d}t} = \frac{1}{T_{\text{d1}}}\sqrt{\delta(1-\zeta)} - \frac{1}{T_{\text{f1}}}\zeta^{5/3}, \quad \frac{\mathrm{d}\delta}{\mathrm{d}t} = \frac{1}{T_{\text{f1}}}\left(\frac{1-\zeta^{5/3}\delta}{1-\zeta}\right). \tag{12}$$

When $B = B_0 + \Delta B$

$$\frac{\mathrm{d}\zeta}{\mathrm{d}t} = \frac{1}{T_{\text{d1}}}\sqrt{\delta(1-\zeta)} - \frac{1}{T_{\text{f2}}}\zeta^{5/3}, \quad \frac{\mathrm{d}\delta}{\mathrm{d}t} = \frac{1}{T_{\text{f2}}}\left(\frac{((B_0+\Delta B)/B_0)^{2/3} - \zeta^{5/3}\delta}{1-\zeta}\right). \tag{13}$$

We nondimensionalise time with the geometric mean of the filling and draining timescales associated with the initial source buoyancy flux. This allows any ΔB to be compared easily to another since the nondimensional time depends only on the initial B, i.e.

$$t = \tau\sqrt{T_{\text{d1}}T_{\text{f1}}} = \frac{SH^{1/3}}{c^{1/4}A^{*(1/2)}}\left(\frac{1}{B_0^{1/3}}\right). \tag{14}$$

When $B = B_0$ (12) becomes

$$\frac{\mathrm{d}\zeta}{\mathrm{d}\tau} = \sqrt{\frac{1}{\mu}}\sqrt{\delta(1-\zeta)} - \sqrt{\mu}\zeta^{5/3}, \quad \frac{\mathrm{d}\delta}{\mathrm{d}\tau} = \sqrt{\mu}\left(\frac{1-\zeta^{5/3}\delta}{1-\zeta}\right), \tag{15}$$

and when $B = B_0 + \Delta B$ (12) becomes

$$\frac{\mathrm{d}\zeta}{\mathrm{d}\tau} = \sqrt{\frac{1}{\mu}}\sqrt{\delta(1-\zeta)} - \sqrt{\mu}\chi\zeta^{5/3}, \quad \frac{\mathrm{d}\delta}{\mathrm{d}\tau} = \sqrt{\mu}\chi\left(\frac{\chi^2 - \zeta^{5/3}\delta}{1-\zeta}\right), \tag{16}$$

Author's personal copy

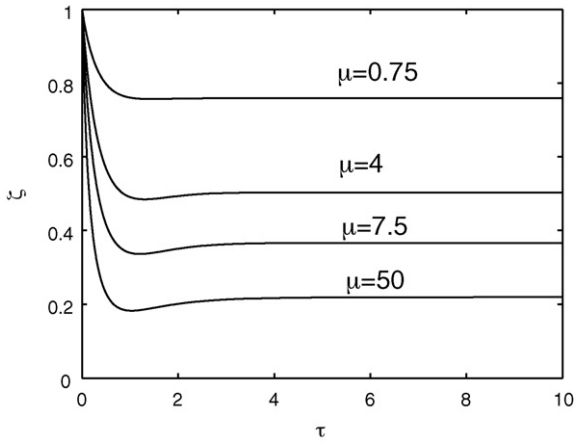

Fig. 2. Initial overshoot beyond steady state predicted by Kaye and Hunt [12] when the source of buoyancy is first turned on for various values of μ. From top to bottom $\mu = 0.75$, 4, 7.5 and 50.

where

$$\mu = \frac{T_{du}}{T_{fu}} = \frac{C^{3/2}H^2}{A^*} \quad \chi = \left(1 + \frac{\Delta B}{B_0}\right)^{1/3}. \tag{17}$$

Eq. (17) defines the system's two governing dimensionless parameters. The ratio μ of the draining and filling time scales is the same as that presented by Kaye and Hunt [12]. It is a nondimensional vent area and solely determines the steady state interface height. The second dimensionless parameter, χ represents the ratio of initial and final source buoyancy fluxes. When $\chi > 1$, B increases and conversely when $\chi < 1$ there is a decrease in B.

The above model is consistent with Kaye and Hunt [12], because as $\Delta B \to 0$, $\chi \to 1$ and Kaye and Hunt's equations are recovered. Fig. 2 reproduces the initial overshoot that they observed when the source of buoyancy is initially switched on. This initial overshoot will be discussed in more detail in the following two sections.

3. Results

In this section we examine the deviations of interface height from the steady state value during transitions from one steady state to the next. Figs. 3 and 4 demonstrate several examples of this deviation.

Fig. 3 illustrates the effect of changing χ for a fixed value of $\mu = 5$. Fig. 3(a) corresponds to a drop in buoyancy (i.e. $\chi < 1$), which causes the interface height to rise initially and then fall back down. Fig. 3(b) shows that for an increase in source buoyancy (i.e. $\chi > 1$) the opposite happens. As χ shifts further from $\chi = 1$, the jump becomes larger. Also, increasing values of χ result in a quicker return to the steady state interface height. A physical explanation for these behaviours is given below.

Fig. 4 illustrates the influence of μ by holding $\chi = 0.5$ fixed and plotting the interface height for various values of μ. The magintude of these jumps is largest for intermediate values of μ corresponding to a steady state interface close to half the height of the room. This behaviour is further illustrated in Fig. 5, which plots the maximum deviation from steady state against μ for various values of χ. Fig. 5(a) corresponds to $\chi < 1$ and (b) to $\chi > 1$.

Figs. 3 and 4 illustrate that as χ deviates further from 1 the size of the jump increases. It should also be noted that a smaller deviation occurs for an increase than an equivalent reduction in B (i.e. $\chi = \chi' > 1$ produces a smaller deviation than $\chi = (1/\chi')$). This is illustrated particularly well in Fig. 5 where the magnitudes in

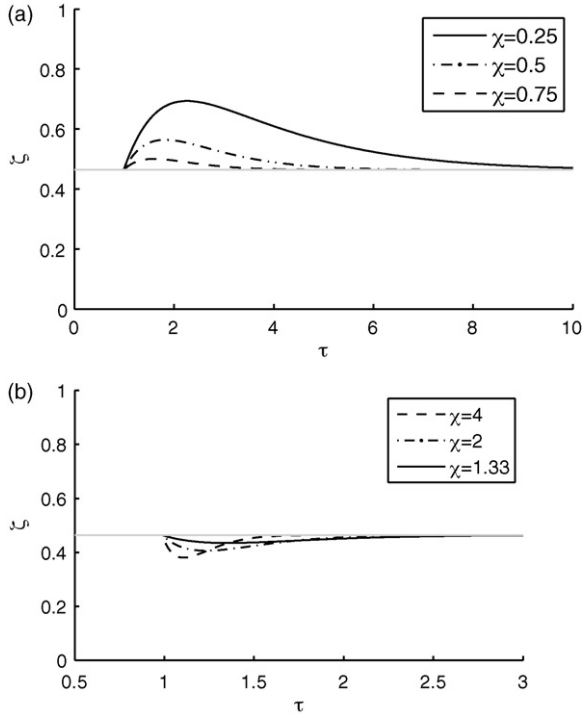

Fig. 3. Interface height for various values of χ and $\mu = 5$: (a) decrease in source buoyancy ($\chi < 1$) and (b) increase in source buoyancy ($\chi > 1$).

Fig. 5(a) are much larger than those in Fig. 5(b). In particular, it becomes increasingly difficult to push the interface down with increasing χ. For example $\chi = 10$, which corresponds roughly to a 1000 times increase in source buoyancy flux only produces a minor change in the amplitude of deviation compared with $\chi = 4$, which corresponds only to a 64-fold increase in source buoyancy.

Now we give some physical insight into the above observations. The adjustment between two steady state interface heights can be explained by referring to [19] and their solution for the volume flux Q of an ideal plume in an unstratified environment given in Eq. (5)

We first consider the situation where the source buoyancy flux is increased. From equation Eq. (5) it is evident that once B is increased the volume flux at the interface will also increase. This causes an imbalance between the flow rate into the upper layer and out of the room, forcing the upper layer to 'fill' and thus the interface to fall. This drop in interface height in turn causes the plume volume flux into the upper layer to decrease. From Eq. (8) we can see that the volume flux out of the space depends on two

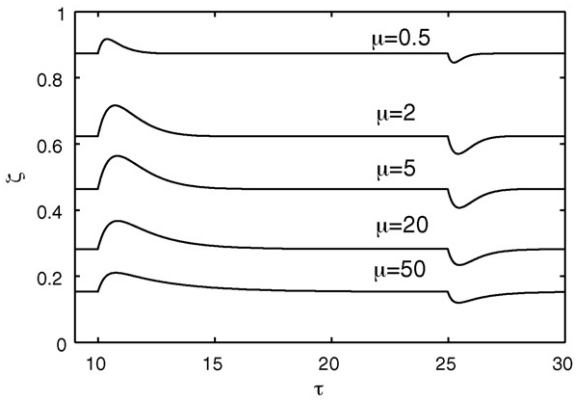

Fig. 4. Interface height for various values of $\mu = 0.5$, 2, 5, 20 and 50 and $\chi = 0.5$.

Author's personal copy

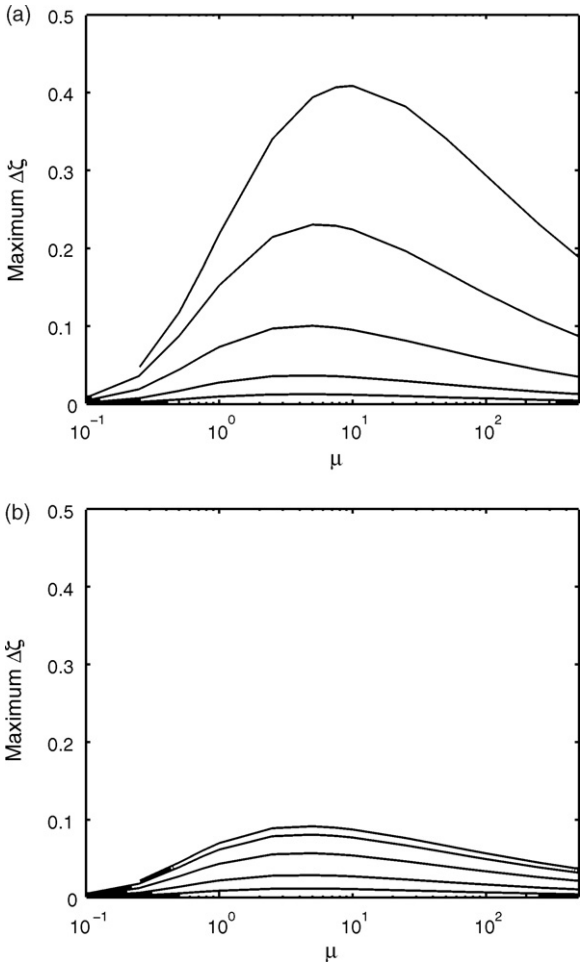

Fig. 5. Maximum deviation of interface from steady state value: (a) $\chi < 1$ (from top to bottom $\chi = 0.1, 0.25, 0.5, 0.75$ and 0.9) and (b) $\chi > 1$ (from top to bottom $\chi = 10$, 4, 2, 1.5 and 1.1) for a range of μ.

things, the buoyancy and depth of the upper layer. Since both these are increasing the volume flux exiting the top of the room will also increase. This, in turn, causes the interface to rise again to its steady state value. It is important to note that the final flow rate through the room is larger than its initial value, now that the source buoyancy flux is higher. The opposite occurs when there is a decrease in B, causing the interface to rise and subsequently fall.

From a mathematical perspective, the second term on the right hand side of Eq. (6) changes when the source buoyancy flux changes. If the source buoyancy flux increases then the left hand side becomes negative, causing the interface to drop and vice versa for a decrease in B.

A typical plot of dimensionless flow rates through the room, q_{out} and q_p, against time in Fig. 6 helps illustrates this phenomenon. When the buoyancy changes there is a sharp change in q_p, while these is some delay in q_{out} reaching its new steady state values. The points where q_p and q_{out} intersect correspond to the turning points (i.e. maximum and minimum overshoot). It is worth noting that the change in q_p is nonmonotonic while that in q_{out} is monotonic. This is because q_p depends on the interface height, which changes nonmonotonically during the transition between steady states (i.e. for an increase in source buoyancy the interface descends and then rises and vice versa for a decrease), while q_{out} depends on the total buoyancy in the upper layer, which varies monotonically from its initial to its next steady state value. Another way to think of this is

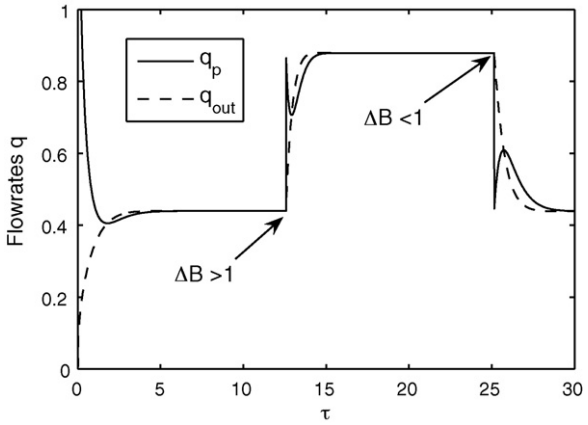

Fig. 6. Flowrates out of the box, q_{out} and flowrate of the plume, q_p across interface against time. The plume is turned on at $\tau = 0$, the the initial steady state is indicated by the constant and equal values of q_p and q_{out}, attained around $\tau = 4$. The buoyancy flux is increased at $\tau = 12$ and the new staey state is achievd at $\tau \approx 15$. Finally, the buoyancy flux is decreased at $\tau = 24$ with the original steady state attained at $\tau = 30$.

that while the steady state interface height is always the same, regardless of the source buoyancy flux, the steady state value of the upper layer buoyancy depends on the strength of the source and is proportional to $B^{2/3}$.

Another important question is why, for an equivalent change in B, the jump from steady state is always larger when the source buoyancy is decreased compared to when it is increased? This behaviour results from the fact that Q_p increases nonlinearly with height ($\propto z^{5/3}$) (see Eq. (5)). Therefore, the imbalance in Q_p and Q_{out} is larger when the interface rises than when it falls, leading to a larger deviation from the state state value.

3.1. No overshoot on the return

As shown in Fig. 2 and first noted by Kaye and Hunt [12], when the source is first turned on the interface descends from the ceiling and 'overshoots' to a point below its ultimate steady state height. When the interface height deviates from its steady state value due to a sudden change in B as studied in this paper, we note that there is no overshoot beyond the steady value when the interface returns. In this section we illustrate mathematically why this happens and subsequently interpret this phenomenon physically. We also discuss the initial overshoot.

When a deviation from the steady state height, ζ_{ss} occurs there must be a maximum/minimum after which it returns to ζ_{ss}. Thus there exists a point, ζ_m where $(d\zeta/d\tau) = 0$ which, from Eq. (16) is given by

$$\frac{\zeta_m^{10/3}}{1-\zeta_m} = \frac{\delta}{\mu^2\chi^2}. \tag{18}$$

Based on observations of many simulations we assume that δ, the dimensionless reduced gravity, is bounded between its initial and final value (i.e. it changes monotonically from its initial to final value with no overshoot beyond its final state). This behaviour is to be expected since the upper layer has a larger steady state buoyancy when B increases and vice versa. From Eqs. (15) and (16) we note that the initial and final steady state nondimensional buoyancies of the upper layer are

$$\delta_{initial} = \zeta^{-5/3}, \quad \delta_{final} = \chi^2\zeta^{-5/3}, \tag{19}$$

Author's personal copy

where χ is greater or less than one depending on whether there is a jump or drop in buoyancy, respectively, i.e.

$$\Delta B > 0 \Rightarrow \zeta^{-5/3} < \delta < \chi^2 \zeta^{-5/3}, \quad \Delta B < 0 \Rightarrow \chi^2 \zeta^{-5/3} < \delta < \zeta^{-5/3}. \tag{20}$$

During the transient, $(\delta/(\mu^2\chi^2))$ the right hand side of Eq. (18), varies from $(1/(\mu^2\chi^2\zeta^{5/3})) \rightarrow (1/(\mu^2\zeta^{5/3}))$. At the turning point $(\mathrm{d}\zeta/\mathrm{d}\tau) = 0$, but $(\mathrm{d}\delta/\mathrm{d}\tau) \neq 0$. Otherwise some other steady state could exist.

For $\Delta B > 0$, $(\mathrm{d}\delta/\mathrm{d}\tau) > 0$, which from Eq. (16) implies

$$\frac{\delta}{\chi^2} < \zeta^{-5/3}. \tag{21}$$

and vice versa for $\Delta B < 0$.

Combining Eqs. (21) and (18) we obtain

$$\Delta B > 0 \Rightarrow \frac{\zeta^{15/3}}{1-\zeta} < \frac{1}{\mu^2}, \tag{22}$$

$$\Delta B < 0 \Rightarrow \frac{\zeta^{15/3}}{1-\zeta} > \frac{1}{\mu^2}. \tag{23}$$

The left hand side, $((\zeta^{15/3})/1-\zeta)$, of the inequalities Eqs. (22) and (23) is a monotonically increasing function in ζ. This explains why a turning point below ζ_{ss} is observed for an increase in buoyancy and vice versa for a drop in buoyancy.

The maximum/minimum value of interface height ζ_m that can be reached during a change in buoyancy can be bounded. For $\Delta B > 0$, combining Eqs. (20) and (18) it can be shown that

$$\frac{1}{\mu^2\chi^2} < \frac{\zeta_m^{15/3}}{1-\zeta_m} < \frac{1}{\mu^2}. \tag{24}$$

A similar inequality exists for $\Delta B < 0$

$$\frac{1}{\mu^2\chi^2} > \frac{\zeta^{15/3}}{1-\zeta} > \frac{1}{\mu^2}. \tag{25}$$

So, for an increase in buoyancy, (24), shows that ζ is always greater than some steady interface height associated with an equivalent $\hat{\mu} = \mu^2\chi^2$, and always less than the steady state value associated with μ, thus explaining why the steady height is never overshot. Similarly, Eq. (25) bounds ζ to remain above the steady height for a drop in buoyancy.

Now that we have answered why no overshoot is observed when settling back to the steady state interface height as a result of a sudden change in buoyancy, it is also important to understand why an overshoot can take place during the establishment of the initial steady state. First, we should note that physically the transition between steady states and the initial overshoot are quite different. The initial 'overshoot' occurs when a source of buoyancy is initially turned on. This corresponds to $\Delta B > 0$. Consequently, from the discussion above, if a turning point does exist, it must exist at a height below the steady state interface height. Therefore, the initial overshoot is similar to the deviation from the steady state height during a sudden increase in source buoyancy as shown in Fig. 7. The main difference is that the initial condition for the interface height is not the steady state value, but rather $\zeta = 1$. In a similar fashion to above we assume δ varies only between its initial and final value

$$1 < \delta < \zeta^{-\frac{5}{3}}. \tag{26}$$

Combining Eqs. (26) and (18) the following inequality is obtained

$$\frac{1}{\mu^2} < \frac{\zeta^{10/3}}{1-\zeta} < \frac{\zeta^{-5/3}}{\mu^2}. \tag{27}$$

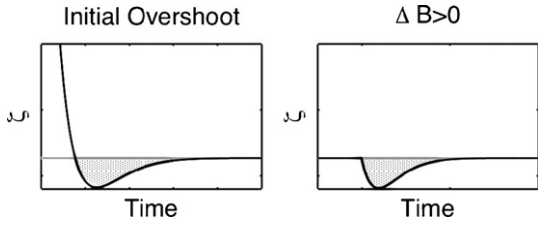

Fig. 7. The initial overshoot is physically similar to the situation where there is a sudden increase in source buoyancy flux.

Note that $(\zeta^{10/3}/1-\zeta)$ is also a monotonically increasing function, which is always greater than $(\zeta^{15/3}/1-\zeta)$. Therefore the solution to $(1/\mu^2) = ((\zeta^{10/3})/1-\zeta)$ lies below ζ_{ss}, allowing ζ to fall below its steady hieght.

4. Comparison with stratified model

A key assumption of the model presented in Section 2 and Section 3 is that the upper layer is considered to be well mixed. In practice, this is not true as the plume will generate a 'filling box' stratification when its buoyancy at the interface is different from the upper layer buoyancy. In this section we develop a Germeles-type model to account for the upper layer stratification and compare the results with those of the well-mixed model.

4.1. Theory

The conservation Eqs. (6) and (8) can be modified to account for the fact that the upper layer is not well mixed. The corresponding conservation equations are

$$\frac{\mathrm{d}h}{\mathrm{d}t} = \frac{A\sqrt{I}}{S} - \frac{CB^{1/3}h^{5/3}}{S}, \tag{28}$$

$$\frac{\mathrm{d}I}{\mathrm{d}t} = \frac{B}{S} - \frac{I\sqrt{I}g'(z=H,t)}{S}, \tag{29}$$

where $I = \int_h^H g' dz$ is the integrated buoyancy in the upper layer.

Defining the average buoyancy of the upper layer $\bar{g}' = \frac{I}{(H-h)}$ and non dimensionalizing as before leads to

$$\frac{\mathrm{d}\zeta}{\mathrm{d}\tau} = \frac{1}{\sqrt{\mu}}\sqrt{\bar{\delta}(1-\zeta)} - \sqrt{\mu}\zeta^{5/3}, \tag{30}$$

$$\frac{\mathrm{d}\bar{\delta}}{\mathrm{d}\tau} = \sqrt{\mu}\left(\frac{1-\bar{\delta}\zeta^{5/3}}{1-\zeta}\right) + \frac{1}{\sqrt{\mu}}\sqrt{\frac{\bar{\delta}}{1-\zeta}}(\bar{\delta} - \delta(\zeta=1)). \tag{31}$$

The only significant difference for the stratified system is the second term in the buoyancy equation Eq. (31) $\left((1/\sqrt{\mu})\sqrt{(\bar{\delta}/1-\zeta)}(\bar{\delta} - \delta(\zeta=1))\right)$. We now ask when this term will be important and when it may be neglected?

Assuming that all other terms are the same order for the well mixed and stratified cases, which does not seem unreasonable, the most important parameter in the above equations is μ. The ratio of the first to second terms in the buoyancy equation Eq. (31) is proportional to μ. As such, for larger values of μ the first term should dominate and the second term becomes negligible, which is indeed what we observe in our simulations below. Large values of μ correspond to small dimensionless vent areas Eq. (17), in which case the upper layer is large. For deep upper layers the contribution of buoyancy from the plume at any given time is small compared to the total amount of buoyancy in the upper layer, whereas for shallow layers this contribution can be significant. As such the effect of stratification becomes less important for large μ.

Author's personal copy

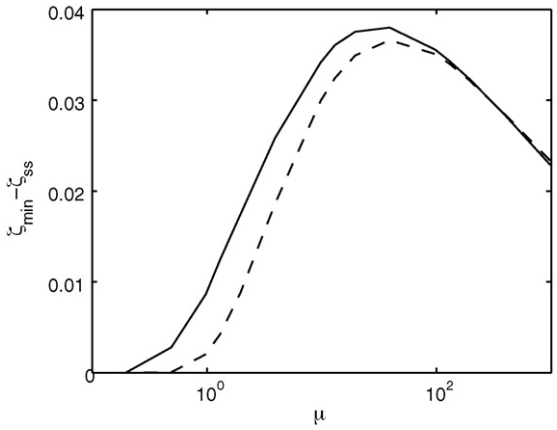

Fig. 8. The size of the initial overshoot beyond steady over a range of μ predicted by the well-mixed model (- -) and the Germeles model (–).

In terms of the time taken to return to steady state, the mixed and stratified systems will also behave differently. For the stratified case the buoyancy extracted from the top of the room will always be the highest. Therefore, if B is increased we expect the system to adjust more slowly for a stratified system than for the mixed case. Conversely, a stratified system should respond more quickly to a decrease in buoyancy. Mathematically, this is represented by the additional term in Eq. (31), which is always negative or zero thus increasing the adjustment time for an increase in buoyancy and decreasing it for a drop.

4.2. Numerical model

In order to determine the impact of this additional term in the buoyancy conservation equation we solve the problem using a Germeles algorithm, which allows a stratification to evolve in the upper layer (see [10] and [5]). A brief description is given here.

The Germeles algorithm is a numerical method that discretizes the ambient density into a finite number of layers. It is assumed that the plume evolves far more rapidly than the ambient density field. Therefore, for any given time step, the plume equations developed by Morton et al. [19] are solved assuming a background density gradient that remains constant over that time step. The equations are solved through the entire height of the room using a 4th order Runge–Kutta algorithm.

Once the plume equations have been solved up to the top of the room, each of the layers in the background is advected downwards with a velocity calculated using the slightly modified version of the Baines and Turner [1] model accounting for the effect of the vent at the top of the room.

At each time step a new layer is added to the room. If the plume has sufficient buoyancy to rise the whole way to the top of the room the new layer is added there. If the plume becomes negatively buoyant at some point the new layer is added at this level of zero buoyancy [13]. In order to account for inflow through the lower vent an additional layer of ambient density is introduced into the bottom of the box at each time step.

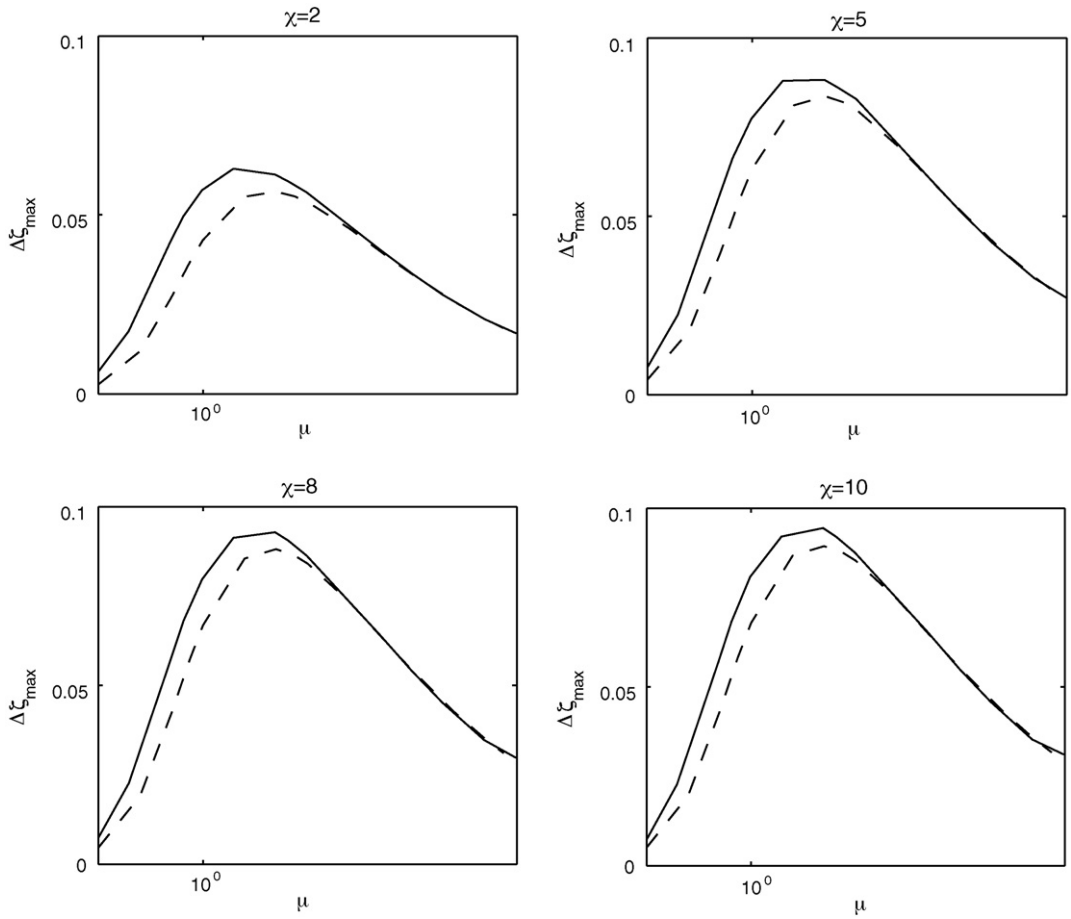

Fig. 9. The maximum deviation from steady state for a rise in B for the well-mixed (- -) vs stratified (–) models for various values of $\chi > 1$.

Author's personal copy

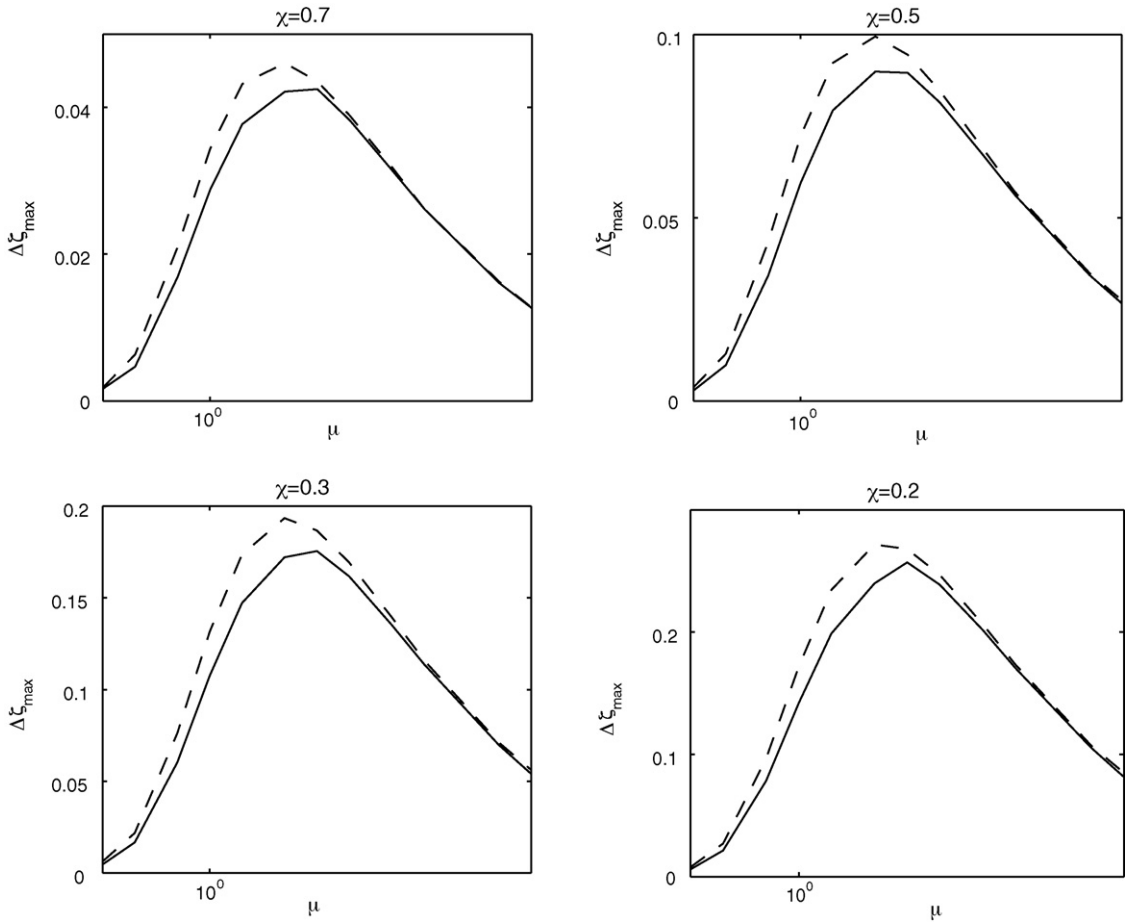

Fig. 10. The maximum deviation from steady state for a drop in B for the well-mixed (- -) vs stratified (–) models for various values of χ.

4.3. Initial overshoot

In this section we examine the initial overshoot when a source of buoyancy is turned on in an initially unstratified box as considered by Kaye and Hunt [12]. Fig. 8 shows the magnitude of the overshoot beyond steady state against μ for both the well-mixed and Germeles models. For all values of μ the overshoot is larger for the stratified case. At large values of μ there is little difference in the size of overshoot since the upper layer is deep as we predicted from the discussion on Eq. (31). For very small values of μ there is almost no overshoot at all. Kaye and Hunt [12] showed that for the well-mixed case no overshoot will occur for $\mu < 0.25$, which we also observe. However for the stratified case an overshoot will exist for even smaller values of μ. Finally, at intermediate values of μ the biggest difference in overshoot occurs. Even so, the largest difference is less than 1% of the height of the room.

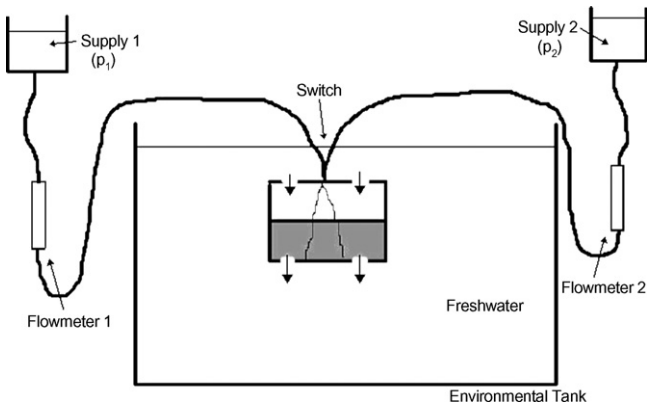

Fig. 11. A schematic of the experiments, showing the ventilated box placed in the large environmental tank. The different buoyancy fluxes are obtained by switching between the two supply tanks.

4.4. Jump in buoyancy

In this section we consider an increase in source buoyancy flux. The system is allowed to evolve to steady state for some initial buoyancy flux. There is a sudden increase in the buoyancy to a value χ^3 times larger than the initial one. The interface height is compared for the well-mixed and Germeles models.

Fig. 9 shows the magnitude of the overshoot beyond the steady state value for both models over a range of μ and for various values of χ. As with the initial overshoot we observe that the difference in predicted overshoot by the well-mixed and Germeles model are insignificant for $\mu > 100$. A difference for values of μ smaller than this does exist. Once again these differences are very small. The maximum overshoot occurs for values of $\mu \sim O(1)$,[1] which corresponds to a steady interface height near the middle of the room. Note also that the magnitude of the overshoot does not appear to change siginificantly for values of χ greater than 5. No matter how much harder the system is forced the interface will not descend further.

[1] close to 5.

Author's personal copy

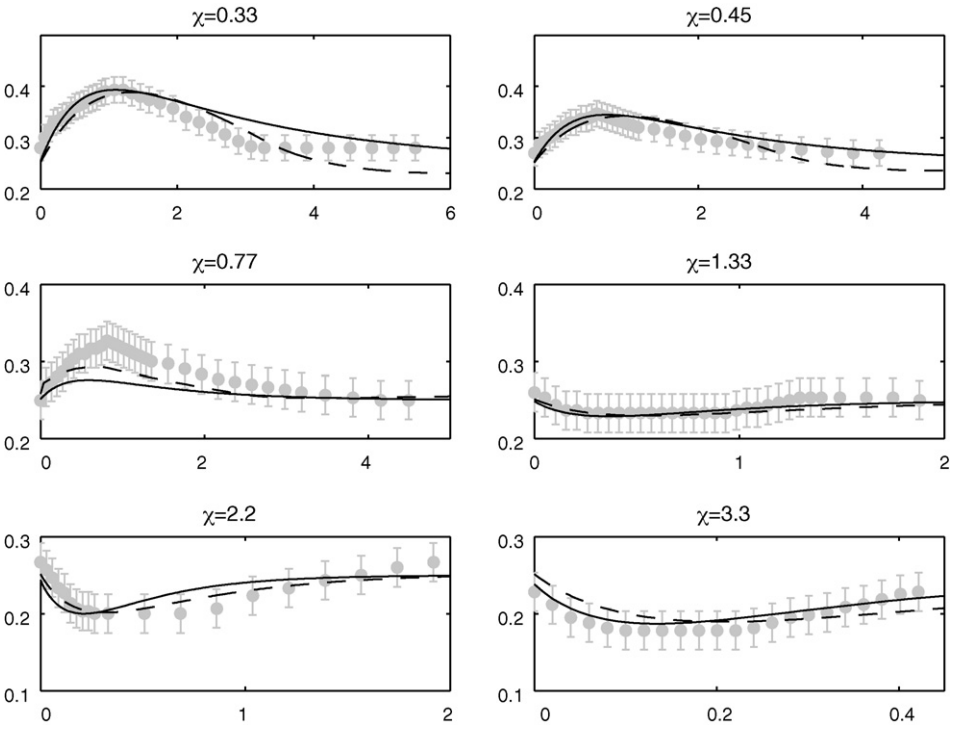

Fig. 12. Interface height vs time for various values of χ at $\zeta = 0.25$. Well mixed (–), stratified (- -), experiment(•). The error bars on the experimental data correspond to typical interface thicknesses.

4.5. Reduction in buoyancy

Here we examine a reduction in source buoyancy flux in the same manner as the last section. Fig. 10 shows the maximum amplitude in the deviation from the steady state interface height for the well-mixed and Germeles model over a range of μ and for various values of χ. Once again we observe a negligible difference in overshoot between the two models for values of $\mu > 100$. Any differences that are observed for smaller values of μ are small, with the largest again occurring around $\mu = 5$. In contrast to the increase in buoyancy flux, the amplitudes do vary significantly with χ.

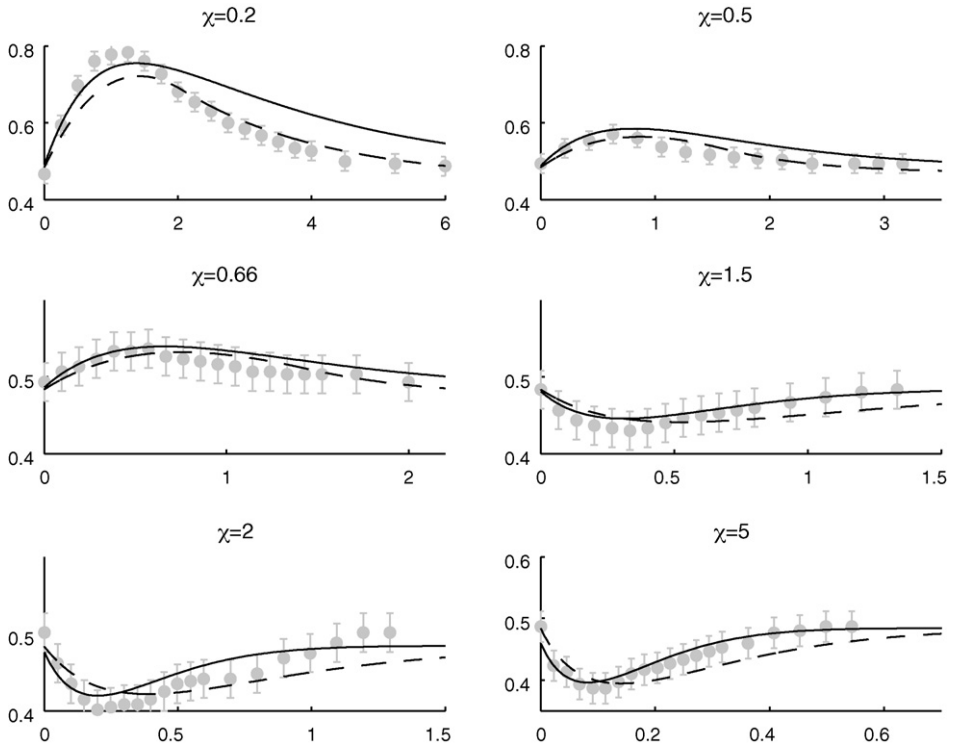

Fig. 13. Interface height vs time for various values of χ at $\zeta = 0.5$. Well mixed (–), stratified (- -), experiment(•). The error bars on the experimental data correspond to typical interface thicknesses.

Author's personal copy

5. Experiments

A sequence of experiments was conducted in order to compare the results to the models described in this paper. The room is represented by a plexiglass tank of dimensions 30 cm × 30 cm ×40 cm, which is submerged in a larger tank that represents the atmosphere (2.4 m × 1.2 m × 1.2 m). The large environmental tank is filled with fresh water. Rather than using heat to change the buoyancy of the fluid we used salt added to water (see Linden [15] for details). Several holes are drilled into the top and bottom of the smaller tank to provide vents to connect the tank to the exterior. Two plume sources, based on the design of Dr. Paul Cooper (see [20]) are placed at the centre of the top of the tank. Since the source in the experiments injects negatively buoyant fluid from the top of the tank it represents an inverted form of the model described so far (Fig. 11).

Two supply tanks, each with fluid of different density can feed one of the plume sources. We switch between the two supplies thus generating a step up or down in source buoyancy flux. Food dye was added to each batch of salt water with a different colour so as to distinguish between the two cases.

From one side of the large tank the apparatus was lit uniformly while recording from the other side using a digital monochrome ccd camera. By measuring the light intensity of the recorded images using the image analysis software, DigImage (see [6]), the interface can be detected as a jump from the light intensity associated with zero dye to that associated with the buoyant layer. Since in practice, the interface is not completely sharp due to finite Peclet number and small disturbances that may exist, a horizontal average, excluding the plume region, of each time frame was taken. The interface is then taken as the point of steepest gradient in light intensity, which is consistent with the method used by Kaye and Hunt [12].

Since the plume sources generate nonideal plumes, virtual origin corrections were calculated with the formulas developed by Kaye and Hunt [11] and then adjusted so that, for each experiment, both plume sources resulted in the same steady interface height.

Figs. 12–14 display the results of these experiments. In all cases the agreement between theory and experiments is good. As predicted in Section 4, values of $\chi < 1$ imply that the Germeles model will reach steady state before the well-mixed model. Conversely for $\chi > 1$ the well mixed model adjusts more quickly. Since in the experiments we neither obtain perfect stratification nor perfect mixing we expect the experimental curves to lie somewhere between the two models, which is, broadly speaking, what we observe.

A measure we use to compare the models to experiments is the prediction of the maximum deviation from the steady state interface (i.e. $\zeta_m - \zeta_{ss}$). Most of the values predicted by the well mixed and stratified models are within ±15% of the experimental values. Larger discrepancies are observed for the $\zeta_{ss} = 0.66$ case and small χ, where the well-mixed model overpredicts the overshoot by close to 50%. This is probably because when there is a decrease in source buoyancy flux there typically little mixing in the upper layer, particularly so for values of $\chi < 0.5$ as shown by Bower [3]. When the plume reaches its level of zero relative buoyancy it becomes a fountain, continues to rise and then falls back before spreading horizontally. Smaller values of $\chi < 1$ (i.e. larger differences in source buoyancy flux) mean that the fountain will have less momentum, rise a smaller height into the region above the level of zero buoyancy and thus cause less mixing, invalidating the well-mixed assumption for the upper layer.

Another region where the differences between theory and experiment were large (between 10 and 40% for both the Germeles and well-mixed models) is when the value of χ is closest to 1 (i.e. $\chi = 0.77$ and $\chi = 1.33$). This is due to the fact that the deviations of the interface from its steady state value tend to be so small as to be close to or even less than the actual thickness of experimental interface as shown by the error bars in Figs. 12–14. In these experiments the thickness of the interface is typically 4–10% of the

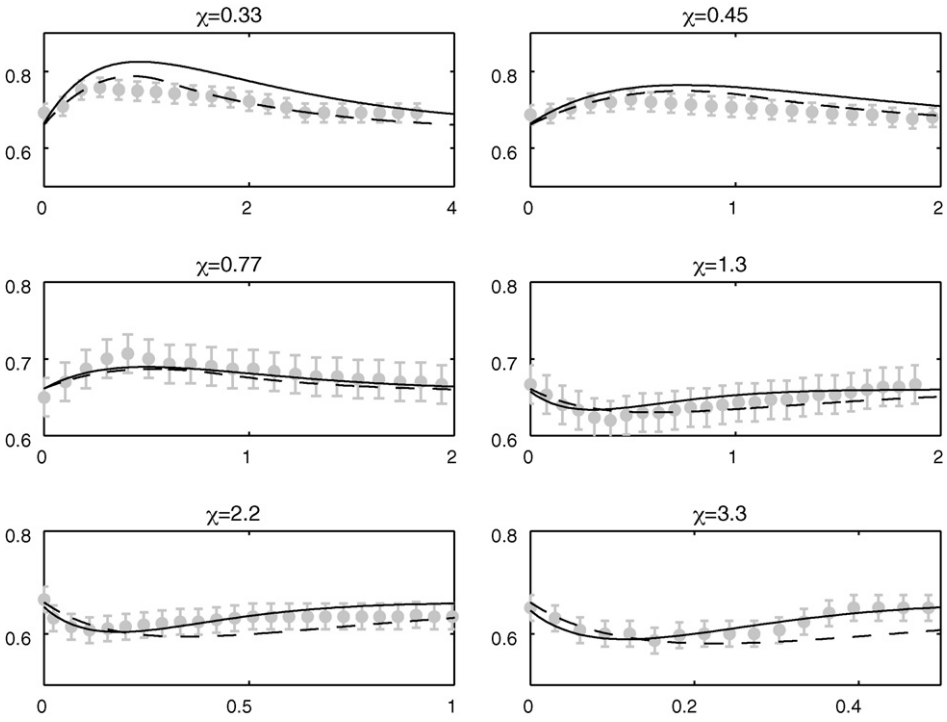

Fig. 14. Interface height vs time for various values of χ at $\zeta = 0.66$. Well mixed (–), stratified (- -), experiment(•). The error bars on the experimental data correspond to typical interface thicknesses.

Author's personal copy

total height of the box. This makes it difficult to pinpoint/define the precise location of the interface during the transient.

Outside these two regions the average error for the well-mixed model was 8.25% with a standard deviation of 4.5%. Excluding only the intermediate values of χ the average error for the Germeles model was 7.8% with a standard deviation of 4%. These values display the good agreement between models and experiments.

Another measure we can use is the time it takes for the interface to return to its steady state value. For $\chi < 1$ the Germeles model predicts this time well-within $\pm 11\%$. However, the well-mixed model performs poorly, overpredicting the time to steady state by as much as 100% for the $\chi = 0.2$ case. Similarly for $\chi > 1$ the well-mixed model predicts this time well-within $\pm 9.5\%$. However, the Germeles model performs poorly the larger χ gets, overpredicting the time to steady state by 80% for the $\chi = 0.33$ case.

It appears that the well-mixed model works better at predicting the interface location when there is an increase in source buoyancy flux, particularly for larger values of χ. This is because when buoyancy is increased, larger values of χ lead to larger volume flow rates and momentum fluxes, causing more mixing in the upper layer, thus strengthening the well mixed approximation. Similarly the Germeles model works best for decreases in buoyancy flux, particularly for smaller values of χ. The reason for this is the lack of mixing that occurs when the plume becomes a fountain as described previously.

6. Summary and conclusions

In this paper we considered a naturally ventilated space containing an isolated source of buoyancy. We developed a mathematical model based on two well-mixed layers and tracked the interface height and buoyancy of the upper layer. The initial descent of the interface height to its steady state value for this model had been previously discussed by [12]. We focused our attention on the affects of a sudden change in buoyancy. We observed a rise and fall back to its steady height of the interface for a decrease in source buoyancy flux. Similarly, we observed a drop and corresponding rise when the source buoyancy flux is increased. After the jump/drop the interface always settles back to the initial steady state height, agreeing with Linden et al. [16]'s observation that the steady interface height is independent of the source buoyancy flux.

We then changed the focus to the assumption that the upper layer is always well mixed. By considering a model that captures stratification (the Germeles model) we compared the predicted deviations of the interface in an attempt to find out what information we lose with this well-mixed assumption. We found that over a wide range of parameters there is very little difference between the two models in terms of predicting the height of the interface. There is a difference in the readjustment timescale depending on whether the heat load is increased or decreased. The stratified system returns to steady state more quickly when there is a decrease in source buoyancy flux, while the well-mixed model will predict a faster time for an increase.

A set of laboratory experiments were conducted to validate our models. In all cases both the well-mixed and Germeles models agreed well with the experiments. Since in the experiments there is neither perfect mixing nor idealised stratification, we expected the interface to lie between the two models, which is generally what was observed. Consequently, since it is both easier and computationally cheaper, we suggest that the well-mixed model is adequate for most practical applications. However, it should not be used in situations where the fine detail of the stratification may be of interest.

In conclusion, we would like to point out that natural displacement ventilation offers several very appealing features.

(1) Natural displacement ventilation is a self-controlling system. As Linden et al. [16] showed the steady state interface location is independent of the strength of heat source. As the amount of heat from sources is increased the flow rate through the space automatically increases.
(2) While we studied both the cases where there is a increase or decrease in source buoyancy flux, from a practical perspective the increasing buoyancy flux scenario is far more interesting. First, most realistic concerns typically arise in situations where there is an increase in the heat load into a room. Second, since in the situation where B is decreased the interface rises and never falls back below the steady height, there is really little need for concern as long as the steady interface height is designed to be at an appropriate level above occupants. Therefore, as long as steady state conditions satisfy any imposed requirements, these requirements will also be satisfied during any transients when the heat load is decreased.
(3) Not only is natural ventilation self-controlling, but additionally the timescale associated with readjustment acts in a favorable manner too. In Section 3 we showed that the larger the increase in source buoyancy flux is, the faster the interface returns to the steady state height. Therefore, in situations where the heat load is increased, there will be a transient during which the interface height can fall into the 'occupied' level. However, the duration of this transient will be shorter that the timescale of the system defined in (14) and will, in fact, be shorter the larger the jump in heat load is.
(4) As mentioned, the only situation which really poses any concern is an increase in heat load. Reassuringly, the amplitude of the deviation from steady state is typically small for situations where this occurs. In Section 4 we showed that the maximum deviation for $\chi = 10$, which corresponds to a 1000-fold increase in source buoyancy flux, is less than 10% of the total height of the room. Therefore any descent of the interface into the occupied layer will not only readjust quickly, but also not penetrate very far.

Acknowldgements

Financial support for Diogo Bolster was provided by the California Energy Commission. We would like to thank Dr. Colm Caulfield and Dr. Morris Flynn for some insightful and engaging discussions on this topic. Additionally, we would like to thank Cade Johnson, an undergraduate student who assisted in running the experiments.

References

[1] W.D. Baines, J.S. Turner, Turbulent buoyant convection from a source in a confined region, Journal of Fluid Mechanics 37 (1969) 51–80.
[2] F. Bauman, T. Webster, H. Jin, W. Lukaschek, C. Benedek, E. Arens, P. Linden, A. Lui, F. Buhl, Dickerhoff. Energy Performance of Underfloor Air Distribution Systems. California Energy Commission, 2007. PIER Building End Use Energy Efficiency Program. Report CEC-500-2007-050.
[3] D. Bower, 2005. Transient Phenomena in Natural Ventilation: Theory and Experiment. Masters Thesis, University of Cambridge.
[4] S.S.S. Cardoso, A.W. Woods, Mixing by a turbulent plume in a confined stratified region, Journal of Fluid Mechanics 250 (1993) 277–305.
[5] C.P. Caulfield, A.W. Woods, The mixing in a room by a localized finite-mass-flux source of buoyancy, Journal of Fluid Mechanics 471 (2002) 33–50.
[6] C. Cenedese, S.B. Dalziel, 1998. Concentration and depth fields determined by the light transmitted through a dyed solution. Proceedings of the 8th International Symposium on Flow Visulaization 8, Paper 061.
[7] D.B. Crawley, L.K. Lawrie, C.O. Pedersen, F.C. Winkelmann, M.J. Witte, R.K. Strand, R.J. Liesen, W.F. Buhl, Y.J. Huang, R.H. Henninger, J. Glazer, D.E. Fisher, D.B. Shirey, B.T. Griffith, P.G. Ellis, L. Gu, EnergyPlus: new, capable, and linked, Journal of Architectural and Planning Research 21 (Winter 2004) 4.

Author's personal copy

[8] D.B. Crawley, L.K. Lawrie, C.O. Pedersen, R.K. Strand, R.J. Liesen, F.C. Winkelmann, W.F. Buhl, Y.J. Huang, A.E. Erdem, D.E. Fisher, M.J. Witte, J. Glazer, EnergyPlus: creating a new-generation building energy simulation program, Energy and Buildings 33 (4) (April 2001) 319–331.
[9] M. Germano, Assessing the natural ventilation potential of the Basel region, Energy and Buildings 39 (2007) 1159–1166.
[10] A.E. Germeles, Forced plumes and mixing of liquids in tanks, Journal of Fluid Mechanics 71 (1975) 601–623.
[11] N.B. Kaye, G.R. Hunt, Virtual origin correction for lazy turbulent plumes, Journal of Fluid Mechanics 435 (2001) 377–396.
[12] N.B. Kaye, G.R. Hunt, Time-dependent flows in an emptying filling box, Journal of Fluid Mechanics 520 (2004) 135–156.
[13] P.D. Killworth, J.S. Turner, Plumes with time-varying buoyancy in a confined region, Geophysical & Astrophysical Fluid Dynamics 20 (1982) 265–291.
[14] M. Kumagai, Turbulent buoyant convection from a source in a confined two-layered region, Journal of Fluid Mechanics 147 (1984) 105–131.
[15] P.F. Linden, The fluid mechanics of natural ventilation, Annual Review of Fluid Mechanics 31 (1999) 201–238.
[16] P.F. Linden, G.F. Lane-Serff, D.A. Smeed, Emptying filling boxes: the fluid mechanics of natural ventilation, Journal of Fluid Mechanics 212 (1990) 309–335.
[17] Q. Liu, P. Linden, An extended model for underfloor air distribution system, in: Proceedings of the SimBuild 2004 Conference, 4–6 August 2004, Boulder, Colorado. IBPSA-USA, 2004.
[18] Q.A. Liu, P.F. Linden, The fluid dynamics of an underfloor air distribution system, Journal of Fluid Mechanics 554 (2006) 323–341.
[19] B.R. Morton, G.I. Taylor, J.S. Turner, Turbulent gravitational convection from maintained and instantaneous sources, Proceedings of the Royal Society A 234 (1956) 1–23.
[20] Hunt, G.R., Cooper, P., Linden, P.F., Thermal stratification produced by jets and plumes in enclosed spaces, Proceedings of Roomvent 2000 the 7th International Conference on Air Distribution in Rooms, Reading UK, In: Awbi, H.B., editor, Reading, Elsevier Science Ltd, 2000, pp. 191–198.